Dynamics of Reaction Separation Processes in the Limit of Chemical Equilibrium

S. Grüner
Institut für Systemdynamik und Regelungstechnik, Universität Stuttgart, Pfaffenwaldring 9, D-70550 Stuttgart, Germany

M. Mangold
Max-Planck-Institut für Dynamik komplexer technischer Systeme, Sandtorstraße 1, D-39106 Magdeburg, Germany

A. Kienle
Lehrstuhl für Automatisierungstechnik/Modellbildung, Otto-von-Guericke-Universität, Universitätsplatz 2, D-39106 Magdeburg, Germany

DOI 10.1002/aic.10686
Published online October 20, 2005 in Wiley InterScience (www.interscience.wiley.com).

A new approach for analyzing and understanding the dynamics of combined reaction separation processes with fast chemical reactions was proposed recently. The approach is based on transformed concentration variables which were first introduced by Doherty and co-workers for the steady-state design of reactive distillation processes. Application was demonstrated for reactive distillation processes and fixed bed, as well as moving-bed chromatographic reactors. The focus was on simple reactions of type $2A \rightleftharpoons B + C$. *This approach is further extended and applied to some real—fairly complex—multireaction systems. Applications to be considered are a reactive enantiomeric separation process in a fixed-bed chromatographic reactor, and an industrial reactive distillation column. Finally, application to membrane reactors is discussed.* © 2005 American Institute of Chemical Engineers *AIChE J,* 52: 1010–1026, 2006
Keywords: reaction separation processes, reactive distillation, chromatographic reactor, membrane reactor, equilibrium theory, nonlinear waves

Introduction

During the past decade, combined reaction separation processes received a lot of attention due to the potential economic benefits compared to conventional technologies, where reaction and separation are carried out in different devices (see, for example, Kulprathipanja,[3] Sundmacher and Kienle,[4] and Sundmacher et al.[5]). Depending on the separation principle, different types of reaction separation processes can be distinguished. Typical examples are reactive distillation processes, which combine chemical reaction with distillation, chromatographic reactors, which combine chemical reaction with chromatographic separation, or membrane reactors, which combine chemical reaction with selective mass transfer across a membrane. In all cases conversion of equilibrium limited chemical reactions can be increased by selective removal of reaction products from the reaction zone. This kind of application can be viewed as a *separation enhanced reaction.*

A second class of combined reaction separation processes, which frequently occurs in practice, are separation processes with potentially reactive mixtures. In this case chemical reaction can be either an unwanted side effect or it can be directly used to achieve a certain separation which is not possible under nonreactive conditions (see, for example, Gaikar and Sharma[6]). The latter represents a *reaction enhanced separation.*

Correspondence concerning this article should be addressed to A. Kienle at kienle@mpi.magdeburg.mpg.de.
A. Kienle is also affiliated with the Max-Planck-Institut für Dynamik Komplexer technischer Systeme, Sandtorstraβe 1, D-39106 Magdeburg, Germany

In all cases a fundamental understanding of the dynamic behavior of these processes is lacking to a large extent. This, however, is a necessary prerequisite for optimal operation and optimal control. Most research in that direction during the last years has focused on reactive distillation due to the industrial importance reactive distillation processes have gained within short time. A review on the present state of the art of dynamics and control of reactive distillation processes was given recently by Kienle and Marquardt.[7] They concluded that even in reactive distillation most investigations have focused on specific processes and only little general results and concepts are available. Even less is known about most of the other reaction separation concepts mentioned earlier. Furthermore, only little comparative studies between different integrated concepts like reactive distillation and chromatographic reactors are available, although these processes are very similar, at least on the conceptual level.

To close this gap, we recently suggested a new theoretical approach.[1] This approach extends classical equilibrium theory for nonreactive separation processes (see, for example, Helfferich and Klein[8] and Rhee et al.[9,10]) to combined reaction separation processes with fast chemical reactions. The new approach makes use of transformed concentration variables, which were first introduced by Doherty and co-workers for the steady-state design of reactive distillation processes.[2] It was shown that these transformed variables can be directly generalized to the dynamic problem[1] and, therefore, also provide useful insight into the dynamic behavior of these processes, which is governed by propagating concentration and temperature fronts. Furthermore, the approach was also extended to other reaction separation processes like fixed and moving-bed chromatographic reactors. For a proof of concept the theory was applied to some ideal ternary reaction systems with a single reversible reaction of type $2A \rightleftharpoons B + C$. In a fully reactive distillation column total conversion is only possible if the reactant has intermediate volatility. In all other cases, the achievable product concentration is limited by reactive azeotropy. Completely analogous behavior was found with the new approach for moving and fixed-bed chromatographic reactors. In this article, this approach is further extended and applied to some real—fairly complex—multireaction systems. For that purpose an extension to multireaction systems is given following the ideas of Ung and Doherty.[11] It is shown that the transformed equilibrium function governs the dynamics of combined reaction separation processes. Furthermore, a general procedure for calculating the transformed equilibrium function and it's derivatives is presented. Practical applications to be considered are a reactive enantiomeric separation process in fixed-bed chromatographic reactor and an industrial reactive distillation column. Finally, also application to membrane reactors is discussed.

Chromatographic Processes

Theoretical background

For an isothermal moving bed adsorber with constant flow rate and negligible axial dispersion the equilibrium model with chemical reaction reads[1]

$$\frac{\partial}{\partial t}\left(\nu\mathbf{q}(\mathbf{c})+\mathbf{c}\right)+\frac{\partial}{\partial z}\left(\mu\mathbf{q}(\mathbf{c})-\mathbf{c}\right)=\boldsymbol{\nu}\tilde{\mathbf{r}}$$

$$\mathbf{q},\mathbf{c}\in R^{N_s},\quad \tilde{\mathbf{r}}\in R^{N_r} \tag{1}$$

where $\mathbf{c}$ and $\mathbf{q}$ are the concentrations of the solid and the fluid phase, which are related by the adsorption isotherms. ν and μ are the volume ratio and the volumetric flow rate ratio of the solid and the fluid phase. Especially, fixed-bed adsorbers are included in this general setting for $\mu = 0$. The axial coordinate z points in the direction of the solid flow. N_s is the number of solutes and N_r is the number of chemical reactions which can take place in the solid and/or the liquid phase. Hence, $\boldsymbol{\nu}$ is an $N_s \times N_r$ matrix of stoichiometric coefficients and $\tilde{\mathbf{r}}$ is a vector of N_r independent reaction rates. This implies that the matrix of stoichiometric coefficients $\boldsymbol{\nu}$ has rank N_r and, therefore, contains an $N_r \times N_r$ invertible submatrix, which is important for what follows.

Remark: If matrix $\boldsymbol{\nu}$ has rank $N < N_r$, not all reaction rates are independent. Hence, we may introduce N new independent reaction rates, which are linear combinations of the old reaction rates. An example was given recently by Aiouache and Goto[12] for the synthesis of tert amyl ethyl ether.

Nonreactive chromatography

In the nonreactive case, $\tilde{\mathbf{r}} = 0$ and Eq. 1 reduces to a set of homogeneous quasilinear partial differential equations of first order according to

$$\frac{\partial}{\partial t}\left(\boldsymbol{\nu}\mathbf{q}(\mathbf{c})+\mathbf{c}\right)+\frac{\partial}{\partial z}\left(\mu\mathbf{q}(\mathbf{c})-\mathbf{c}\right)=\mathbf{0} \tag{2}$$

For this type of problem a comprehensive mathematical theory with application to fixed-bed and moving-bed chromatographic processes was given by Rhee et al.[9,10] Equivalent results were obtained with a different approach, based on physical insight by Hellferich and Klein.[8] A nice review of the latter approach was given more recently in a series of articles.[13–15]

According to the theory, solutions of Eq. 2 depend on the adsorption isotherm $\mathbf{q}(\mathbf{c})$, which is the dominating nonlinearity in the system, and the operating conditions, which are related to the boundary and initial conditions of Eq. 2 and the flow rate ratio μ. Let us briefly summarize some of the main results, we shall need in the remainder. Emphasis in the books and papers cited earlier is on Langmuir systems, that is, systems whose sorption equilibrium can be described by the competitive Langmuir isotherm

$$q_i=\frac{a_i c_i}{1+\sum_{k=1}^{N_s} b_k c_k},\quad i=1,\ldots N_s \tag{3}$$

For simplicity, consider first a fixed-bed chromatographic column. For Langmuir systems, any concentration step change introduced at the entrance of an initially unloaded chromatographic column will be resolved in a sequence of at most N_s shock waves s_i as illustrated in the upper right diagram of Figure 1 for a two solute system. A reverse step change is introduced, when a totally loaded column is purged with pure solvent. This reverse step change is resolved in at most N_s

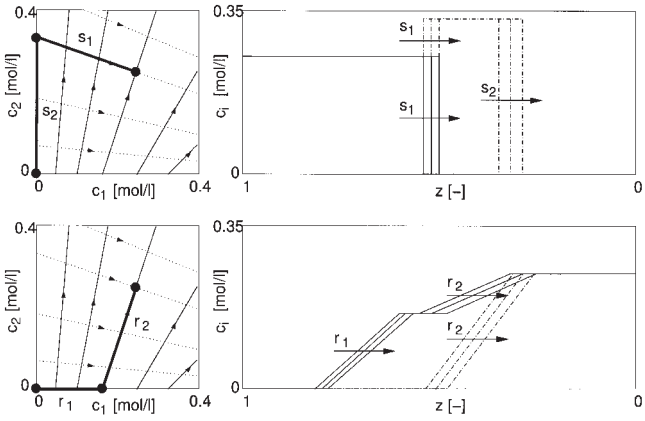

Figure 1. Wave solutions for Langmuir systems.

Step changes of the concentration in the inlet. Top right: concentration profiles for the loading of an initially empty bed. Bottom right: purge of a completely loaded bed with pure solvent. Solid line—c_1, dashed dotted line—c_2. Left: Corresponding wave solutions in the hodograph space.

dispersive or spreading waves r_i as illustrated in the bottom right diagram of Figure 1.

These solutions are easily constructed in the concentration phase space or the so-called hodograph space. Both types of wave solution represent N_s time-invariant curves in the hodograph space. For Langmuir systems shock and spreading wave curves are straight lines in the hodograph space and, therefore, coincide. They do not depend on the operating conditions. They are given by the right eigenvectors $\mathbf{r}_k$ of the Jacobian matrix $\partial\mathbf{q}/\partial\mathbf{c}$, which comprises the partial derivatives of the adsorption isotherms with respect to the fluid-phase concentrations

$$\frac{\partial \mathbf{q}}{\partial \mathbf{c}}\,\mathbf{r}_k = \lambda_k \mathbf{r}_k, \quad k = 1, \ldots N_s \tag{4}$$

The initial condition and the boundary condition of a step change represent points in this hodograph space. Any wave solution can be constructed from the pathgrid of the eigenvectors by connecting the initial point with the boundary point as illustrated on the left of Figure 1. The construction is done in the following way: We start at the point, which represents the boundary condition, and follow the path belonging to the smaller eigenvalue of Eq. 4. The paths belonging to the smaller eigenvalues are indicated by the dotted lines. Afterwards, we switch to the solid line running through the point, which represents the initial condition. The solid lines represent the paths belonging to the larger eigenvalue of Eq. 4. If we follow the path in the direction of the arrows, the corresponding wave solution is a spreading wave and a shock wave, otherwise.

Any pulse injection to an unloaded bed can be interpreted as a sequence of the two-step changes discussed earlier. This situation is illustrated in Figure 2 and gives rise to N_s shock waves in the front, and N_s spreading waves in the rear. According to the rules of elementary wave interactions these are finally resolved into N_s pure component pulses with a shock in front and a spreading wave in the rear.[10]

Additional complexity will rise for systems with more complicated sorption isotherms, involving inflection points and adsorptivity reversal (azeotropy). For these type of mixtures spreading waves and shock waves are usually represented by curved lines in the hodograph space and will, therefore, not coincide. Spreading waves follow from the eigenvectors of the phase equilibrium, and do not depend on the operating conditions. In contrast to this shock waves follow from the global material balances across the shock and will, therefore, depend on the operating conditions. However, as proposed by Helfferich and Klein[8] at least a qualitative picture of the overall situation can be gained from the pathgrid of the eigenvectors. The reason for that is that the shock wave curves, and the eigenvectors are always tangent at the starting point. New phenomena for non-Langmuirian systems are: the existence of combined wave solutions for adsorption isotherms with inflection points and limitations on feasible product composition due to adsorptivity reversal similar to azeotropic distillation. Examples for the latter were treated by Basmadijan et al.,[16–18] among others.

Reactive chromatography

In the reactive case the nonhomogeneous Eq. 1 has to be considered. For sufficiently fast chemical reactions, reaction equilibrium can be assumed in addition to phase equilibrium. The chemical equilibrium conditions represent N_r algebraic constraints, which reduce the dynamic degrees of freedom of the system to $N_s - N_r$.[1] In the limit of reaction equilibrium the kinetic rate expressions for the reaction rates become indeterminate and have to be eliminated from the balance Eq. 1. Following the ideas of Ung and Doherty,[11] this is achieved by choosing N_r reference components and splitting the concentration vectors accordingly into two parts

$$\mathbf{c} = [\mathbf{c}^I, \mathbf{c}^{II}], \quad \mathbf{q} = [\mathbf{q}^I, \mathbf{q}^{II}], \quad \mathbf{c}^I, \mathbf{q}^I \in R^{N_r}, \quad \mathbf{c}^{II}, \mathbf{q}^{II} \in R^{N_s - N_r} \tag{5}$$

An analogous splitting is introduced for the matrix of stoichioimetric coefficients

$$\boldsymbol{\nu} = [\boldsymbol{\nu}^I, \boldsymbol{\nu}^{II}] \tag{6}$$

where $\boldsymbol{\nu}^I$ has dimensions $N_r \times N_r$ and $\boldsymbol{\nu}^{II}$ has dimensions $(N_s - N_r) \times N_r$. By solving the first N_r equations of Eq. 1 for

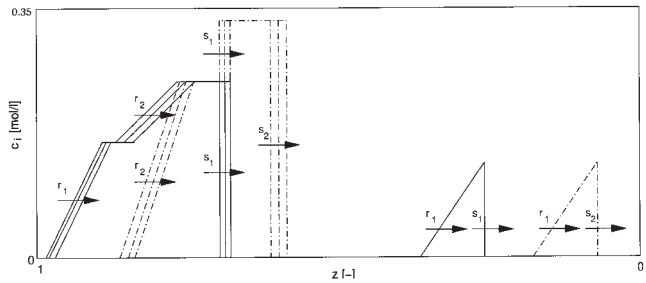

Figure 2. Wave solutions for Langmuir systems.

Two snapshots at different times after a pulse injection are shown. At the left: shortly after injection. The front has resolved into two shocks, while the back is just about to resolve into two rarefaction waves. Further to the right: The pulse has resolved into two separate pulses containing pure components. Solid line—c_1, dashed dotted line—c_2.

the unknown reaction rates and substituting them into the remaining $N_s - N_r$ equations, the following reduced set of equations is obtained

$$\frac{\partial}{\partial t}(\nu\mathbf{Q} + \mathbf{C}) + \frac{\partial}{\partial z}(\mu\mathbf{Q} - \mathbf{C}) = 0 \tag{7}$$

with transformed concentration variables according to

$$\mathbf{C} = \mathbf{c}^{II} - \boldsymbol{\nu}^{II}(\boldsymbol{\nu}^{I})^{-1}\mathbf{c}^{I}, \quad \mathbf{Q} = \mathbf{q}^{II} - \boldsymbol{\nu}^{II}(\boldsymbol{\nu}^{I})^{-1}\mathbf{q}^{I}, \quad \mathbf{C}, \mathbf{Q} \in R^{N_s - N_r} \tag{8}$$

Equation 7 is completely analogous to the nonreactive problem Eq. 2. Hence, in the limit of reaction equilibrium the reactive problem is completely equivalent to a nonreactive problem in a reduced set of transformed concentration variables. Obviously, solutions of Eq. 7 will now depend on the properties of the transformed equilibrium function **Q**, which includes information about the phase *and* the reaction equilibrium. In analogy to the nonreactive case Eq. 2, the transformed equilibrium function **Q** has to be interpreted as a function of the transformed fluid phase concentration **C**, that is, **Q**(**C**). However, only in special cases this function can be calculated explicitly.[1] Nevertheless, this function, its eigenvectors and eigenvalues are easily calculated numerically with some suitable DAE-solver. The outline of a fairly general procedure is given in Appendix A. It applies to any number of components, any number of reactions, and arbitrary phase and reaction equilibrium relations. With this, an analogous pathgrid of eigenvectors can be generated, and all sorts of solutions are readily constructed by a simple graphical procedure like in the nonreactive case in Figure 1. We shall illustrate the procedure in the remainder with a fairly complex application example.

Application to the Separation of Binaphthol Enantiomers

In the following, we consider the separation of enantiomers through achiral chromatography. Enantiomers are isomers which behave like image and mirror image. They play an important role in pharmaceutical industry. Usually they are separated with special chiral stationary phases, which have a high specific selectivity for one of the enantiomers. However, in some cases a separation effect can also be observed if an achiral stationary phase is used, which has no specific selectivity for one of the enantiomers. At first glance this is rather surprising, but can be explained with the presence of some chemical reactions taking place.

This problem was studied by Baiocchi et al.[19] among others, for binaphthol enantiomers. In particular, they made the following experimental observations. When a pulse with racemic composition of the enantiomers (that is, a mixture with equal amount of both enantiomers) was injected to the column, no separation occurred. In contrast to this, in all cases where a nonracemic mixture was injected, the pulse split into a first fraction with pure excess enantiomers and into a second fraction with almost racemic composition. This separation effect can be explained with the presence of some dimerization reactions. According to Baciocchi et al.,[19] we shall denote the enantiomers with *S* and *R*. The enantiomers can build three different dimers according to

$$R + R \rightleftharpoons RR \tag{9}$$

$$S + S \rightleftharpoons SS \tag{10}$$

$$R + S \rightleftharpoons RS \tag{11}$$

Dimers *RR* and *SS* are called homochiral dimers, whereas the mixed dimer *RS* is called a heterochiral dimer. A fraction of pure enantiomer is always a mixture of the monomer and the corresponding homochiral dimer, but does not contain any heterochiral dimer. It was shown, that the separation of the excess enantiomer of a nonracemic feed mixture is the combination of two effects,[20] the difference in reaction equilibrium constants of the homo- and heterochiral dimerization reaction, and the difference in the adsorptivity of the homo- and heterochiral dimers.

The earlier experimental observations were reproduced by Baciocchi et al.[19] with numerical simulation. Their model was based on the following assumptions:

(1) Phase equilibrium was assumed between the solid and the fluid phase, and modeled with competitive Bi-Langmuir adsorption isotherm. With the notation introduced in this article, the adsorption isotherm reads to

$$q_i = \frac{h_i c_i}{G} + \frac{a_i c_i}{B}, \quad i = R, S, RR, SS, RS \tag{12}$$

with

$$G = 1 + g_1(c_R + c_S) + g_2(c_{RR} + c_{SS}) + g_3 c_{RS}$$
$$B = 1 + b_1(c_R + c_S) + b_2(c_{RR} + c_{SS}) + b_3 c_{RS}$$

Equal selectivity was assumed between all monomers and homochiral dimers, and a large difference in selectivity between homo- and heterochiral dimers.

(2) Furthermore, it was assumed that the dimerization reactions take only place in the liquid phase. The reactions are rather fast and, therefore, reaction equilibrium was assumed. Like Baciocchi et al.[19] the following relation between the equilibrium constants of the homo- and the heterochiral dimerization was applied in this study

$$K_{\text{hetero}} = 2K_{\text{homo}} \tag{13}$$

This constraint was relaxed in a more recent article by Baciocchi et al.[21] It is worth noting, that an extension of the subsequent analysis to this more general case is straight forward, but beyond the scope of this article.

With simultaneous phase and reaction equilibrium the system has only two dynamic degrees of freedom (5 solutes–3 chemical equilibria). If the dimers are taken as reference components the following definition of the transformed concentration variables is found from Eq. 8

$$C_R = c_R + 2c_{RR} + c_{RS}, \quad C_S = c_S + 2c_{SS} + c_{RS} \tag{14}$$

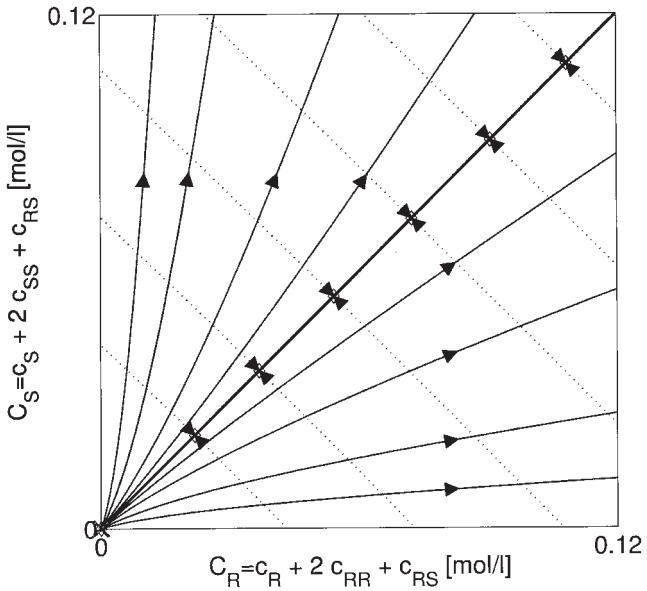

Figure 3. Pathgrid of the eigenvectors in the hodograph space of the transformed concentration variables for the binaphthol system.

$$Q_R = q_R + 2q_{RR} + q_{RS}, \quad Q_S = q_S + 2q_{SS} + q_{RS} \qquad (15)$$

It should be noted, that this is consistent with the model formulation of Baciocchi et al.[19] However, their focus was on simulation,[19] that is, numerical solution of the underlying partial differential equations for given boundary and initial conditions. In contrast to this, we will use the equilibrium theory developed above to predict solutions for any piecewise constant initial and boundary conditions at a single glance. Moreover, this will provide some deeper insight into the problem and uncover additional interesting features of the asymptotic pulse responses.

The construction of wave solutions is based on the pathgrid of the eigenvectors of the combined phase and reaction equilibrium in the hodograph space. The pathgrid was calculated with the methods described in Appendix A. The pathgrid in terms of transformed concentration variables C_S and C_R according to Eq. 14 is shown in Figure 3. In this representation the x-axis represents pure R enantiomer consisting of the corresponding monomers and dimers and the y-axis represents pure S enantiomer. Racemic compositions lie on the bisection line. The topology of the pathgrid in Figure 3 shows some remarkable differences to the pathgrid of the nonreactive Langmuir system that was shown in Figure 1. In particular, all solid lines corresponding to the fast waves for the larger eigenvalue intersect at the origin. There, the characteristic velocities of the fast and slow waves coincide. Such a singularity is called an umbilic point in the mathematical literature,[22] and a watershed point in the chromatographic literature.[8] Furthermore, the pathgrid is symmetric with respect to the bisection line $C_S = C_R$. This is obvious from the physical point of view because both enantiomers behave the same. The slow wave curves for the smaller eigenvalue are parallel, and change their orientation at the bisection line.

For a nonracemic feed, the wave solution for the loading of initially unloaded bed will always consist of two shocks. The first fraction contains the enantiomeric excess, which is thereby separated from the rest. This situation is illustrated in the second row of Figure 4a and 4c, which are symmetric due to the symmetry of the pathgrid in Figure 3. Therein, the origin represents the initial condition. For a racemic feed mixture, any feed concentration lies on the bisection line and can be connected to the origin by a single shock and, therefore, no separation is possible as illustrated in the second row of Figure 4b. Furthermore, the solid and dashed curves coincide.

A different situation occurs if purging of an initially loaded bed with pure solvent is considered as illustrated in the third row of Figure 4. Here, no difference between racemic and nonracemic initial conditions exist. The origin represents the pure solvent purge, which can be connected with any initial condition by a single wave curve. Consequently, any wave solution of this kind will consist of a single spreading wave moving jointly for both enantiomers and, therefore, no separation occurs. For any racemic composition the composition profiles of both components will coincide. It should be noted that the funny shape of the spreading waves in Figure 4 is the consequence of a strong variation of the characteristic velocity in the lower left part of the wave, and a weak variation in the upper right part of the wave.

Like in the nonreactive case, a pulse injection of the feed can be viewed as the combination of a positive and a negative step change of the feed concentration. The positive step change corresponds to the scenario shown in the second row of Figure 4, and the negative step change corresponds to the scenario in the third row of Figure 4. After some wave interactions the final pulse patterns as illustrated in Figure 5 are obtained. These pulse patterns have some special features, which are clearly different from the nonreactive case illustrated in Figure 2. For a racemic mixture the pattern consists of a single pulse, which has the same velocity and shape for both components. For a nonracemic mixture, the solution consist of a first fraction with pure excess enantiomer and a second fraction, containing both enantiomers. In contrast to the nonreactive case in Figure 2, both fractions stick together and will never separate as shown in Figure 5a and 5c. This is consistent with the observations of Baciocchi et al.[19] and comes from the special topology of the pathgrid in Figure 3. Due to the intersection of all solid lines at the origin, pulse patterns through the origin include only three waves as further illustrated by the triangles in the left diagram of Figure 6. However, as shown before in Figure 2, any isolated pulse is formed by at least two waves. So, the formation of two isolated pulses requires a minimum number of four waves, which is therefore not possible in the present case. Furthermore, due to the symmetry of the pathgrid, the solutions in Figure 5a and 5c, are again perfectly symmetric.

The influence of the feed composition is illustrated in Figure 6. The front pulse with pure excess enantiomer is getting narrower as the feed composition is approaching the bisection line—corresponding to a racemic composition—and finally disappears for a racemic feed mixture.

So far, focus was on separation of a nonracemic mixture with an initially unloaded column. Another option which can be studied is the separation of a racemic mixture with a column

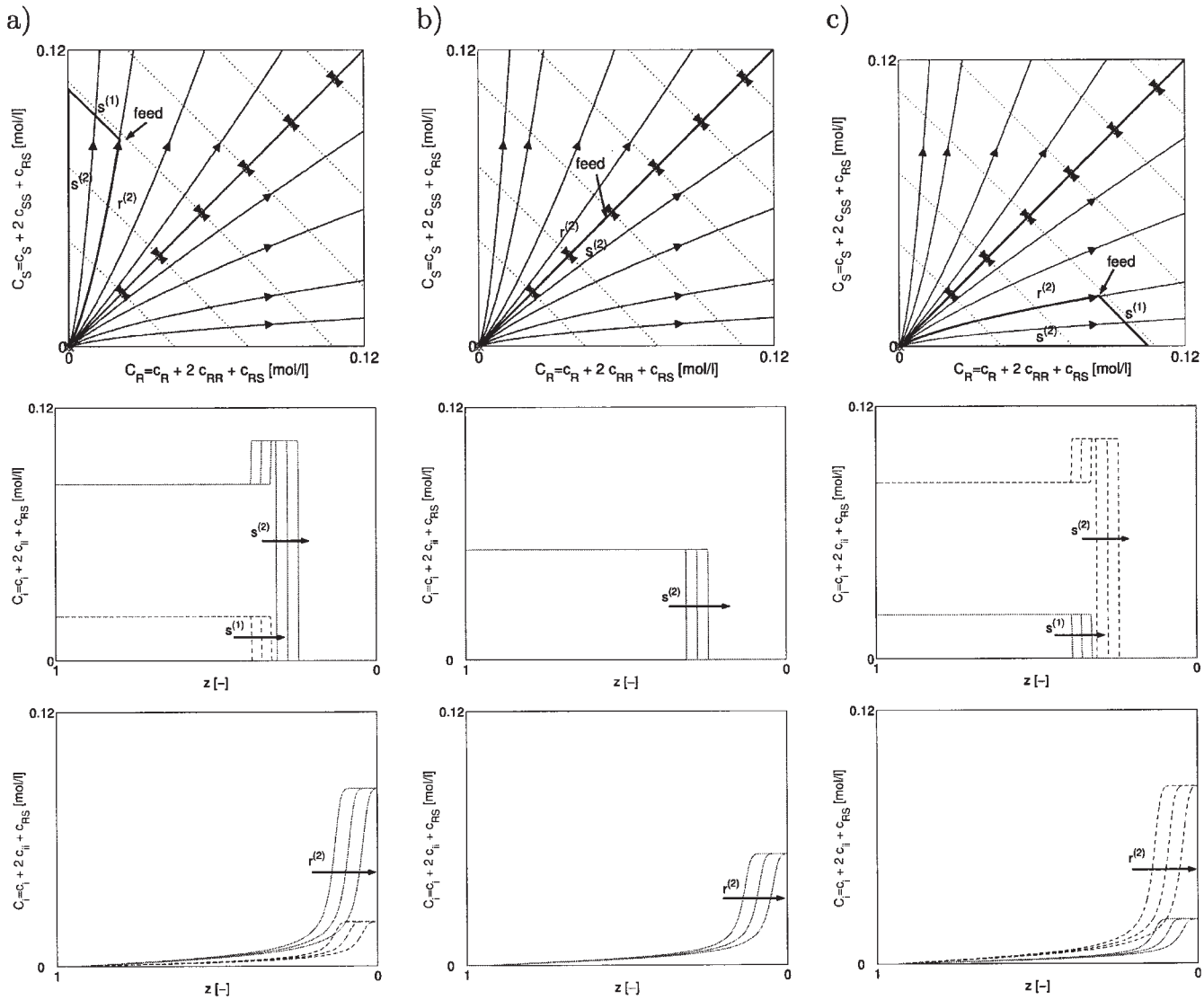

Figure 4. Wave solutions for the binaphthol system in transformed concentration variables.

Step changes of the concentration in the inlet. Top row: wave solutions in the hodograph space. Center row: concentration profiles for the loading of an initially empty bed. Bottom row: purge of a completely loaded bed with pure solvent. Solid line—C_R, dashed line—C_S. (a) nonracemic feed with an excess of the *S* enantiomer, (b) racemic feed, and (c) nonracemic feed with an excess of the *R* enantiomer.

that is preloaded with one of the enantiomers. This situation is illustrated in Figure 7 for different preloadings. In contrast to Figure 6, the initial pulse pattern in the hodograph space now consists of a quadrangle compared to the triangles in Figure 6. This implies that the wave solution now consists of four instead of three waves as in Figure 6. Consequently, in contrast to Figure 6, the final pulse pattern will now consist of two pulses, which will be separated if the column is long enough. Similar like in Figure 6, the front pulse with pure excess enantiomer is getting smaller and smaller and will finally disappear as the preloading of the bed tends to zero.

Although the practical relevance of this last example is low, it nicely illustrates how the methods introduced in this article can be used to develop and discuss alternative modes of operation quite rapidly.

Distillation Processes

Theoretical background

For a single section of a distillation column with constant molar flow rates and holdups, constant pressure and negligible axial dispersion the equilibrium model with chemical reaction reads[1]

$$\frac{\partial}{\partial t}\left(\varepsilon\mathbf{y}(\mathbf{x})+\mathbf{x}\right)+\frac{\partial}{\partial z}\left(\frac{1}{A}\mathbf{y}(\mathbf{x})-\mathbf{x}\right)=\boldsymbol{\nu}\mathbf{r}$$

$$\mathbf{y},\mathbf{x}\in R^{N_c-1},\quad \mathbf{r}\in R^{N_r} \tag{16}$$

Here, the axial coordinate z points in the direction of the vapor flow. It is worth noting that this model formulation is

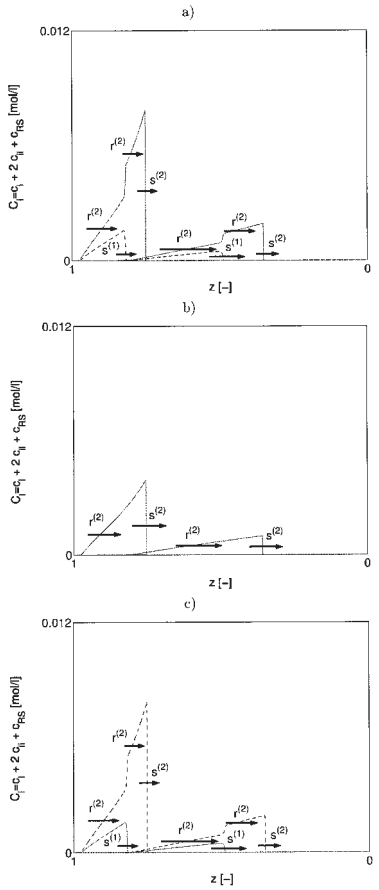

Figure 5. Pulse responses in a fixed bed chromatographic reactor for the different cases in Figure 4.

Transformed concentration variables: Solid line—C_R, dashed line—C_S.

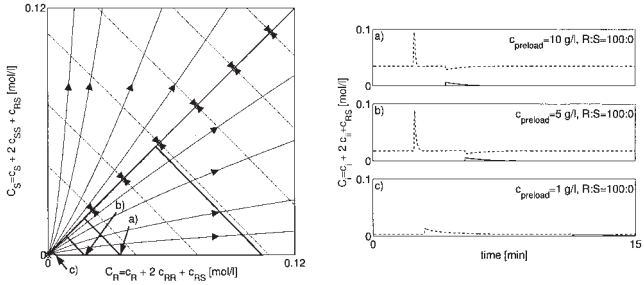

Figure 7. Influence of preloading on the pulse of a racemic feed.

Left: Wave solutions in the hodograph space of the transformed concentration variables. Right: Chromatograms of the transformed concentration. Solid line—C_R, dashed line—C_S.

completely analogous to the moving-bed adsorber (Eq. 1). In this formulation, **x** and **y** are the mole fractions of the liquid and the vapor phase, which are related by the vapor liquid equilibrium. ε and A are the ratios of the molar holdups and the convective molar flow rates in both phases. N_c is the number of components. Because the mole fractions **x** and **y** have to satisfy corresponding summation conditions, only $N_c - 1$ material balances are taken into account. Again, N_r is the number of independent chemical reactions. In reactive distillation, chemical reactions will mainly take place in the liquid phase. However, side reactions in the vapor phase can also occur.

Nonreactive distillation

In the nonreactive case, Eq. 16 reduce to a homogeneous problem again

$$\frac{\partial}{\partial t}\left(\varepsilon \mathbf{y}(\mathbf{x}) + \mathbf{x}\right) + \frac{\partial}{\partial z}\left(\frac{1}{A}\mathbf{y}(\mathbf{x}) - \mathbf{x}\right) = \mathbf{0} \tag{17}$$

Solutions for this type of problem will now consist of at most $N_c - 1$ waves in each column section, if the Jacobian of the equilibrium function has a full set of independent eigenvalues and eigenvectors.[23] This is always satisfied for ideal and moderately nonideal mixtures. For highly nonideal mixtures multiple eigenvalues may arise and more than $N_c - 1$ waves are possible.[23,24] At steady state, at most one of these wave fronts is located in the middle of the column section, while the others are located at the system boundaries where they can overlap for mixtures with more than three components. After some disturbance, the waves may travel through the column depending on the sign and size of the disturbance until they settle down to a new steady state. An illustration was given by Kienle.[25] For ideal mixtures all waves are of the constant pattern wave type, whereas for nonideal mixtures combined wave solutions are also possible.

Construction of wave solutions for binary mixtures in the

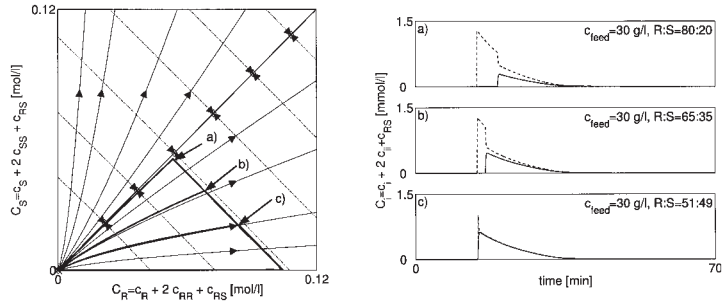

Figure 6. Influence of feed composition on the pulse response of an initially unloaded bed.

Left diagram: Wave solutions in the hodograph space of the transformed concentration variables. Right diagram: Chromatograms of the transformed concentration. Solid line—C_R, dashed line—C_S.

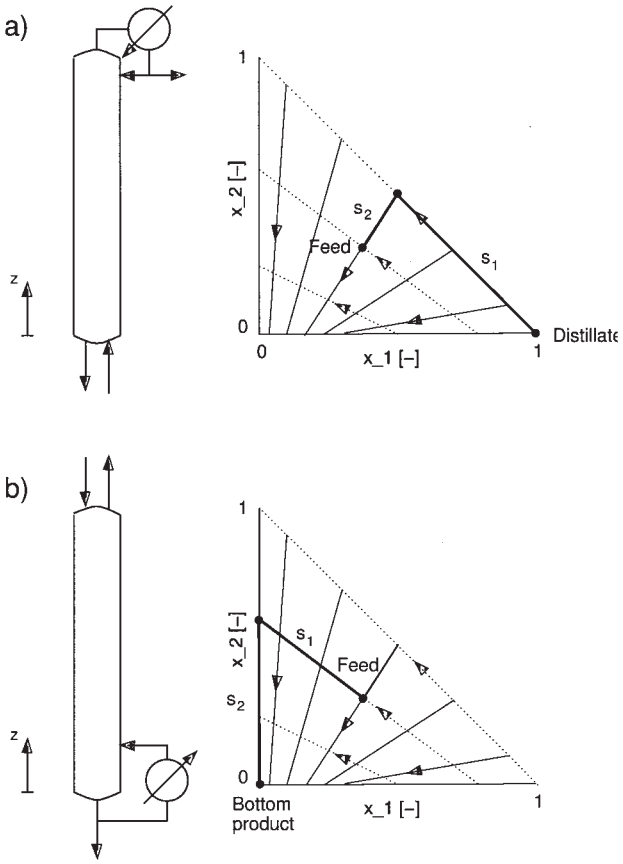

Figure 8. Wave solutions in the hodograph space for ideal ternary distillation with constant relative volatilities: (a) rectifying column, and (b) stripping column.

McCabe–Thiele diagram was discussed by Grüner and Kienle.[1] In the multicomponent case we may proceed similar to the previous section. This is illustrated in Figure 8 for an ideal ternary mixture with constant relative volatilities. Like in the case of Langmuir isotherms shock and spreading wave curves in the hodograph space are straight lines and coincide. In a retifying section the boundary condition at the top is represented by the pure lightest boiling component, which is the component 1 in Figure 8a. The lower boundary condition is given by the liquid concentration which is in equilibrium with the given vapor feed. The wave solution consists of two shocks, connecting the two boundary conditions according to the rules discussed in the previous section. The intermediate plateau represents a binary mixture of light and intermediate boiling component. In general the solution consists of at most $N_c - 2$ intermediate plateaus, where the components successively vanish in the order of increasing volatility.[23] The reverse behavior can be found in a stripping column illustrated in Figure 8b. Here, the concentration of the liquid feed represents the boundary condition at the top, and the pure heaviest boiling component represents the boundary condition at the bottom. Again, the solution will contain at most $N_c - 2$ intermediate plateaus, where the components vanish in the order of decreasing volatility from the top to the bottom.

For nonideal mixtures constant pattern wave and spreading wave curves in the hodograph space are no longer straight lines and are, therefore, different. However, as argued in the previous section, the pathgrid of the eigenvectors may also serve as an approximate solution for shock waves. For azeotropic mixtures, the "lightest boiling component" is the corresponding unstable node of the residue curve map,[26] whereas the "heaviest boiling component" is represented by the corresponding stable node of the residue curve map.

Reactive distillation

In the reactive case, we proceed completely analogous to section. Again, reaction equilibrium is assumed for fast chemical reactions. Upon elimination of the unknown reaction rates the following reduced set of equations in transformed concentration variables is obtained

$$\frac{\partial}{\partial t}(\varepsilon \mathbf{Y} + \mathbf{X}) + \frac{\partial}{\partial z}\left(\frac{1}{A}\mathbf{Y} - \mathbf{X}\right) = 0 \tag{18}$$

with transformed concentration variables according to

$$\mathbf{X} = \mathbf{x}^{II} - \boldsymbol{\nu}^{II}(\boldsymbol{\nu}^{I})^{-1}\mathbf{x}^{I}, \quad \mathbf{Y} = \mathbf{y}^{II} - \boldsymbol{\nu}^{II}(\boldsymbol{\nu}^{I})^{-1}\mathbf{y}^{I}, \quad \mathbf{X}, \mathbf{Y} \in R^{N_c - 1 - N_r} \tag{19}$$

Again, Eq. 18 is equivalent to a nonreactive problem in a reduced set of transformed concentration variables. In analogy to the nonreactive case (Eq. 17) solutions of Eq. 18 will depend on the properties of the transformed equilibrium function $\mathbf{Y}(\mathbf{X})$, and its eigenvalues and eigenvectors. These can be calculated with the methods discussed in Appendix A. In the remainder application is illustrated for a fairly complex industrial reactive distillation process.

Remark 1: In the case of equimolar reactions the above definition of the transformed concentration variables is completely equivalent to the definition of Ung and Doherty,[11] who treated the corresponding steady state problem. However, it is worth noting, that the general definition for nonequimolar reaction rates as given by Ung and Doherty[11] for the steady state case is *not* readily extended to the dynamic problem considered here.*

Remark 2: In reactive distillation a nonequimolar reaction necessarily implies a variable molar flow rate of the corresponding phase. In reactive chromatography, this effect can often be neglected due to the presence of a solvent. In some cases the amount of reacting species is small compared to the amount of solvent. A typical example is the binaphthol separation process discussed earlier. In other cases the solvent is one of the reactants, which also comes in large excess. Typical examples are the ester hydrolysis systems considered by Mai et al.[27] In both cases the bulk flow rates are only little affected by a nonequimolar reaction.

Application to an Industrial Reactive Distillation Process

Consider the reactive distillation column illustrated in Figure 9. In this column a mixture of two reactants *B* and *C* is

* For a discussion of this fact the reader is also referred to the conclusion section.

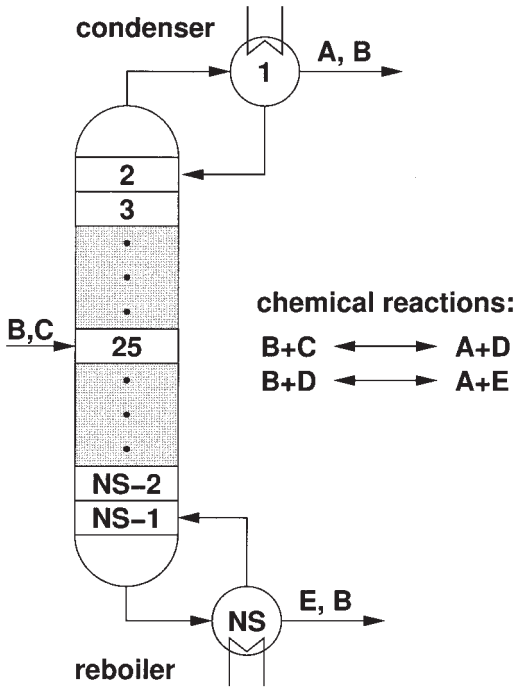

Figure 9. Industrial reactive distillation column.

converted in two successive reversible equimolar reactions to products A and E. The light boiling product A is obtained at the top of the column and the heavy boiling product E is obtained in the bottom of the column. The reaction mixture contains a total number of five components. The (nonreactive) phase equilibrium of the system is highly nonideal including 4 binary azeotropes with a temperature minimum, and 1 binary azeotropes with a temperature maximum. Furthermore, it was found that the column is operated close to chemical equilibrium.

As already reported by Grüner and Kienle,[1] this column shows distinct wave propagation characteristics, which will be analyzed in some more detail in this section with the methods introduced earlier.

Assuming that both chemical reactions are in equilibrium the number of dynamic degrees of freedom of the system $N_c - 1 - N_r$ is equal to two. If, for example, the two reactants B and C are chosen as reference components to eliminate the unknown reaction rates the following definition of the two transformed concentration variables is obtained

$$X_1 = x_A + x_B, \quad X_2 = x_E - x_C + x_B \tag{20}$$

$$Y_1 = y_A + y_B, \quad Y_2 = y_E - y_C + y_B \tag{21}$$

The corresponding concentration phase space is a trapezoid. This is similar to the xylene reactive separation problem treated by Ung and Doherty.[11] The reactive residue curve map of the present system is illustrated in Figure 10. In this representation the origin and the four corners represent the pure components. The nonreactive pairs A/B and C/D show nonreactive azeotropes. The other nonreactive azeotropes mentioned earlier occur for potentially reactive mixtures and do not survive in the reactive system. However, due to the chemical reaction a new binary reactive azeotrope arises on the A/E edge, and a new ternary reactive saddle azeotrope close to this. This complex geometry gives rise to five distillation regions (I → V in Figure 10), which differ with respect to the starting or the end point of the trajectories, that is, the possible top and bottom products in a fully reactive distillation column of infinite length with infinite reflux. In this case, the column is operated in region II of Figure 10. At steady state, the top product is close to the nonreactive A/B azeotrope, whereas the bottom product lies on the B/E edge.

The corresponding pathgrid of the eigenvectors of the transformed equilibrium function is illustrated in Figure 11. It was calculated numerically with the methods presented in Appendix A. The arrows along the wave curves point in the direction of increasing characteristic velocity. It is shown in Figure 11 that the gradient of the characteristic velocity along the curves may change quite often it's sign, in particular along the solid lines close to the upper right corner. In addition to the wave curves the distillation boundaries from Figure 10 are also indicated in Figure 11. Hence, Figure 11 can be used to construct any wave solution for any piecewise constant initial and boundary conditions. This is illustrated in Figure 11 for a pure stripping column. The liquid feed at the upper end of the stripping column is the nominal feed of the column in Figure 9. The wave solution consists of a first piece connecting the feed with the E/B edge and a second piece connecting the point of intersection with the E/B edge with the E/B azeotrope, which represents the stable node in this distillation region. Along the first piece the gradient of the characteristic velocity is changing

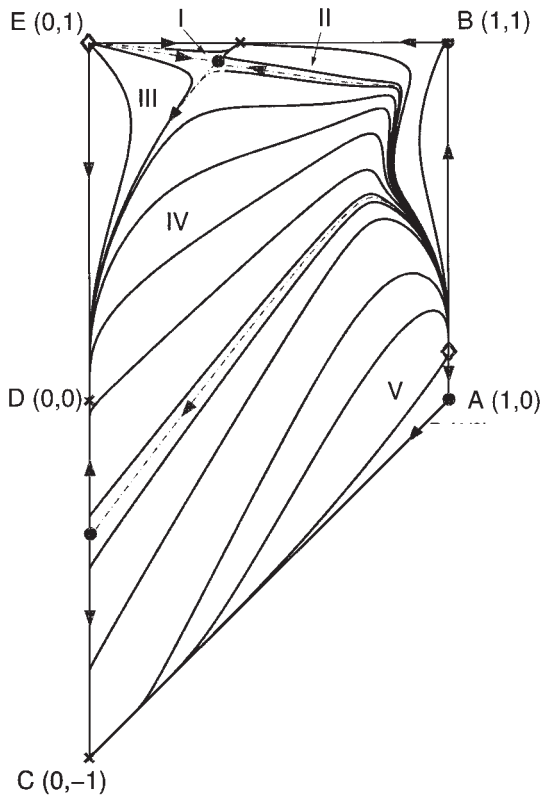

Figure 10. Reactive residue curve map corresponding to Figure 9.

Solid circles—saddle points, diamond—unstable node, cross—stable node.

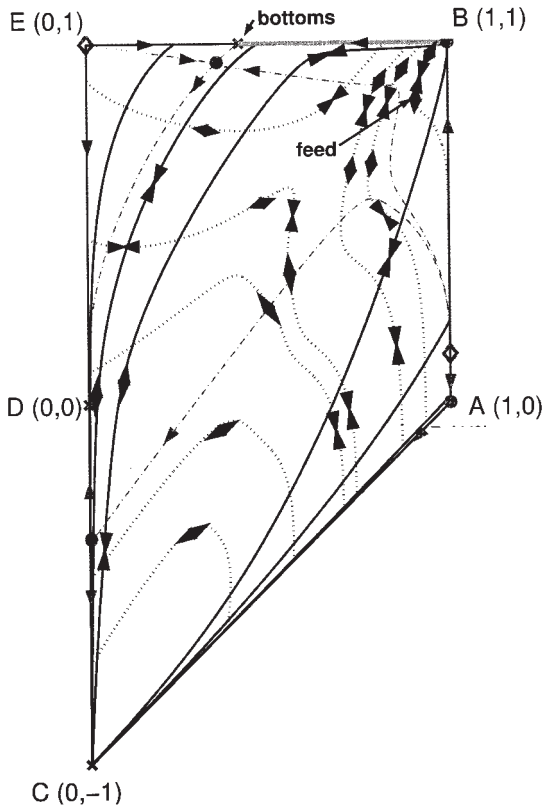

Figure 11. Pathgrid of the eigenvectors in the hodograph space of the transformed concentration variables for the reactive distillation system illustrated in Figure 9.

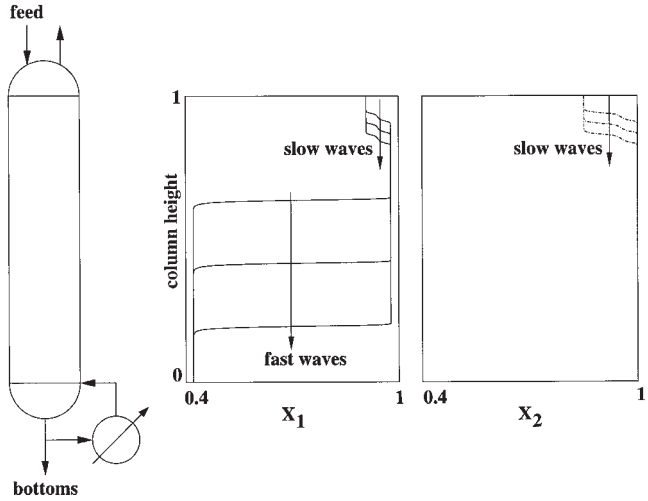

Figure 12. Dynamic transient behavior of the transformed concentration variables for the stripping section of the reactive distillation system illustrated in Figure 9.

twice indicating that the corresponding wave is a combined wave which consists of two shocks which are connected by a spreading wave. Instead, the second piece represents a single shock wave. These predictions are confirmed by dynamic simulation in Figure 12. Figure 12 shows the column profiles of the transformed concentration variables X_1 and X_2 as the column approaches steady state from a constant initial concentration profile with composition of the A/B azeotrope.

Membrane Processes

In the following section possible extensions of the concepts to membrane reactors will be discussed. In contrast to the previous examples the assumption of phase equilibrium is no longer acceptable for membrane reactors and has to be relaxed. The treatment to be discussed subsequently follows closely the concepts, which were recently proposed by Huang et al.[28] for reactive membrane pervaporation processes. There, the time dependent behavior of a well-mixed open reactive pervaporation process was studied. The process is described by a set of ordinary differential equations, which can also be used to describe the steady state behavior of a spatially distributed parameter membrane reactor. Here, the concepts are extended to the dynamics of spatially distributed membrane reactors, which are described by systems of partial differential equations.

Two main operation schemes of membrane reactors can be distinguished:[29] selective product removal Figure 13a and distributed injection of reactants Figure 13b. In the first case, the membrane is used to increase the conversion of an equilibrium limited reaction by separating the reaction products. This requires the membrane to be selectively permeable for one of the products. It is applicable, for example, to dehydrogenations. In the second case, the concentration of one of the reactants is controlled by feeding it across the membrane. This may increase the yield and selectivity of an intermediate product of consecutive reactions like selective oxidations. In this section, focus is on the first case, that is, product extraction. Transformed variables are used to analyze the limiting case of reaction equilibrium, corresponding

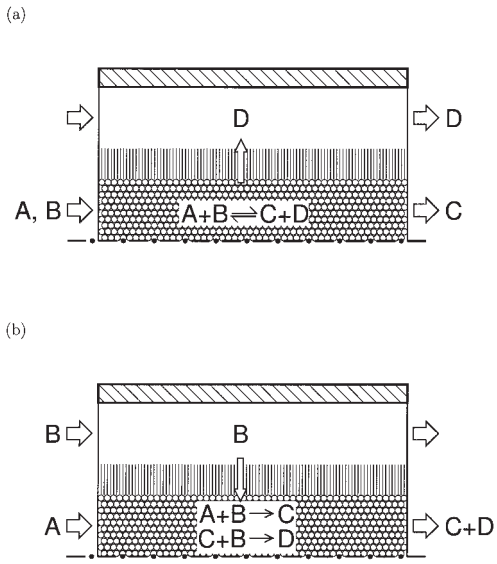

Figure 13. Two different operation principles of membrane reactors: (a) selective withdrawal of products, and (b) distributed injection of reactants.

to an infinitely fast reaction. The second case will be treated elsewhere.

Theoretical Background

Consider a membrane reactor as illustrated in Figure 13a consisting of an inner tube with a supply of reactants, and an outer tube with sweep gas supply. In the following, it is assumed that the sweep gas flow is very high, so that all material which is transported across the membrane is readily removed and thus the concentration of all reacting species in the sweep gas channel is equal to zero. Furthermore, the following assumptions are made

- isothermal operation
- negligible axial dispersion
- constant pressure
- equimolar reactions

The last assumption is in line with the previous treatment of reactive distillation processes and chromatographic reactors. It simplifies the mathematics a lot and, therefore, helps to focus more on the physical interpretation of the results.

With the earlier assumptions the model equations follow from the material balances of $N_c - 1$ independent species on the reaction side. In dimensionless form the model equations read

$$\frac{\partial \mathbf{x}}{\partial t} + \frac{\partial (v\mathbf{x})}{\partial z} = -\mathbf{j}(\mathbf{x}) + \boldsymbol{\nu}\mathbf{r}(\mathbf{x}), \tag{22}$$

$$\frac{\partial v}{\partial z} = -j_{tot}, \tag{23}$$

with

$$j_{tot} = \sum_{i=1}^{N_c} j_i, \quad \mathbf{x} \in R^{N_c - 1}, \quad \mathbf{j} \in R^{N_c}, \quad \mathbf{r} \in R^{N_r}$$

with dimensionless spatial and time coordinates z, t defined by

$$z = \frac{\bar{z}}{l}, \quad t = \frac{\bar{t} v_0}{l} \tag{24}$$

and the dimensionless velocity

$$v = \frac{\bar{v}}{v_0} \tag{25}$$

Here, the axial coordinate z points in the direction of the fluid flow. It is worth noting, that we have only $N_c - 1$ independent species but N_c independent fluxes across the phase boundary, that is, we can specify N_c component fluxes j_i or $N_c - 1$ component fluxes, and the total flow rate j_{tot} instead. In the remainder, the first approach will be used.

In view of the total material balance (Eq. 23) the component material balances (Eq. 22) can be simplified to

$$\frac{\partial \mathbf{x}}{\partial t} + v\frac{\partial \mathbf{x}}{\partial z} = -\mathbf{j}(\mathbf{x}) + \mathbf{x}j_{tot} + \boldsymbol{\nu}\mathbf{r}(\mathbf{x}) \tag{26}$$

Main differences to reactive distillation processes and chromatographic reactors treated above are (1) the variable flow rate in the inner tube, which is a consequence of the nonnegligible amount of material transported across the membrane into the outer tube, and (2) the finite mass transfer resistance of the membrane, which can not be neglected in contrast to the other processes considered earlier.

Nonreactive Membrane Separation

In the nonreactive case the reaction rate $\mathbf{r}$ is equal to zero and the model equations read

$$\frac{\partial \mathbf{x}}{\partial t} + v\frac{\partial \mathbf{x}}{\partial z} = -\mathbf{j}(\mathbf{x}) + \mathbf{x}j_{tot} \tag{27}$$

$$\frac{\partial v}{\partial z} = -j_{\text{tot}} \tag{28}$$

Due to the finite mass transport kinetics across the membrane this is even in the nonreactive case a system of nonhomogeneous quasilinear partial differential equations, whose properties will crucially depend on the flux function $\mathbf{j}(\mathbf{x})$. For simplicity, we will focus on a simple diagonal flux function according to

$$j_i = \beta_i x_i, \quad i = 1, \ldots N_c \tag{29}$$

A discussion of more complicated cases was given for example by Krishna and Wesselingh.[30]

Let us illustrate the behavior of the nonreactive membrane separation system with a simple example. Consider a binary mixture with components A, B. Let us assume that the membrane has highest permeability for component A and let us first focus on the steady-state behavior of such a process. Let Eq. 27 be the material balance of component A. According to Eq. 27 the slope of the steady state profile depends on the relative flux ratio j_A/j_{tot}, and it's dependence on the concentration x_A. If j_A/j_{tot} is larger than x_A, then the concentration is decreasing and vice versa. Hence, the qualitative behavior is easily extracted from a diagram of the flux ratio j_A/j_{tot} vs. concentration x_A as illustrated on the right side of Figure 14. This diagram is the analogon to the well-known McCabe–Thiele diagram for distillation processes and nicely illustrates the influence of mass-transfer resistance.[31] For the simple relation in Eq. 29 we find

$$\frac{j_i}{j_{\text{tot}}} = \frac{\beta_i x_i}{\sum_{k=1}^{N_c} \beta_k x_k}, \quad i = 1, \ldots N_c - 1 \tag{30}$$

which is equivalent to the vapor liquid equilibrium for mixtures with constant relative volatilities. Since the membrane has highest permeability for component A the flux ratio j_A/j_{tot} is always larger than x_A. Therefore, the concentration of A is monotonically decreasing in the inner membrane tube, and will tend to zero for an infinitely long tube. In a similar way the

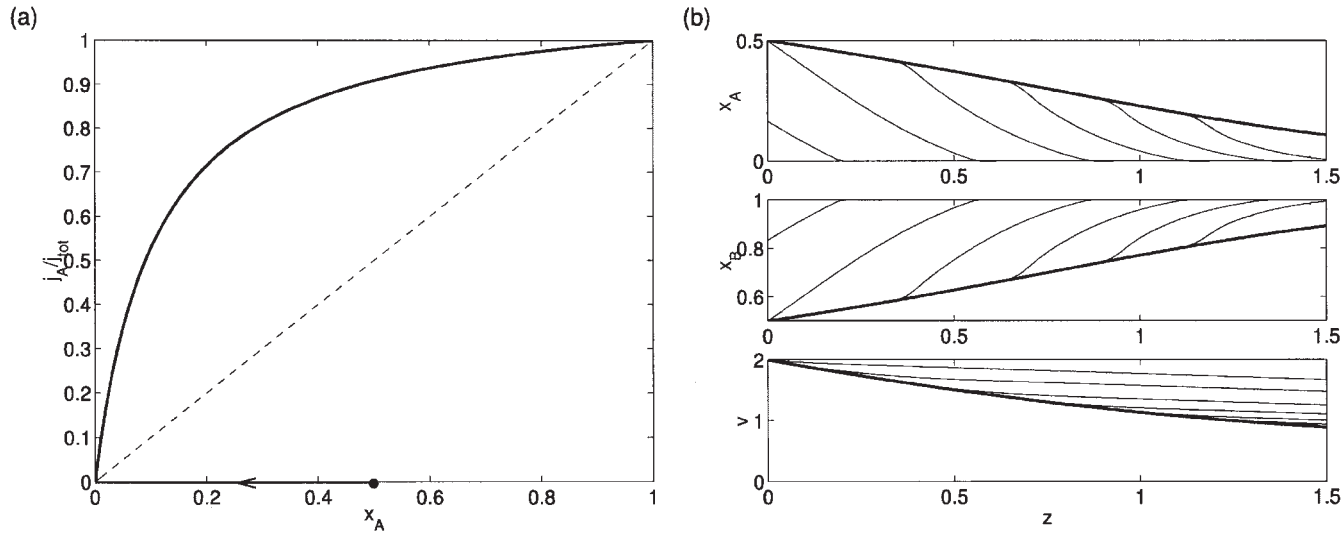

Figure 14. Nonreactive membrane separation.

Parameters: $\beta_A = 2$; $\beta_B = 0.2$. (a) Flux rate ratio of A through membrane vs. x_A, (b) response to an input ramp of $x_{A,in}$ as shown in Figure 15. Thin lines = transient solutions at $t = 0.2, 0.4, \ldots, 1.2$, bold lines = steady state solution.

flow rate in the inner tube is decreased monotonically and tends to zero. For a tube of finite length a finite flow rate and a finite concentration between is obtained.

The dynamic transient behavior during startup is illustrated on the left side of Figure 14. Like in reactive distillation and reactive chromatography, the transient behavior is governed by traveling fronts. In this case, these waves can only propagate downstream.

Furthermore, since the velocity in the inner tube is decreasing continuously from the inlet to the outlet by material transport across the membrane, concentration values closer to the inlet will move with higher velocity than concentration values closer to the outlet. Consequently, all waves are self sharpening in Figure 14.

Alternatively, also inlet concentration disturbances of the steady state profile could be considered. Due to the inhomogeneity in Eq. 27 the concentration waves will travel downstream on the nonconstant initial profile as the system undergoes a transient from the old to a new monotonically decreasing steady state.

The same type of dynamics can be observed in the multicomponent case. In contrast to distillation and chromatographic processes treated in the previous section, any step disturbance will be resolved into a single front traveling jointly for all components. This is due to the fact that all balance equations share the same transport velocity v.

Membrane Reactors

In the reactive case, the full blown Eq. 26 together with the total material balance (Eq. 23) has to be considered. For fast chemical reactions, again, reaction equilibrium can be assumed and the corresponding model equations are again obtained by elimination of the unknown reaction rates from the material balances (Eq. 26).

The reduced set of equations is obtained in the following form

$$\frac{\partial \mathbf{X}}{\partial t} + v\frac{\partial \mathbf{X}}{\partial z} = -\mathbf{J}(\mathbf{x}) + \mathbf{X}J_{\text{tot}} \tag{31}$$

$$\frac{\partial v}{\partial z} = -J_{\text{tot}} \tag{32}$$

with transformed concentration and flux variables according to

$$\mathbf{X} = \mathbf{x}^{II} - \boldsymbol{\nu}^{II}(\boldsymbol{\nu}^{I})^{-1}\mathbf{x}^{I}, \quad \mathbf{J} = \mathbf{j}^{II} - \tilde{\boldsymbol{\nu}}^{II}(\boldsymbol{\nu}^{I})^{-1}\mathbf{j}^{I}$$

$$\mathbf{X} \in R^{N_c-1-N_r}, \quad \mathbf{J} \in R^{N_c-N_r} \tag{33}$$

It is worth noting, that like in the nonreactive case, the dimension of the flux vector exceeds the dimension of the concentration vector by one. Consequently, the dimension of $\mathbf{j}^{II}$ exceeds the dimension of $\mathbf{x}^{II}$ by one, and matrix $\tilde{\boldsymbol{\nu}}^{II}$ consists of matrix $\boldsymbol{\nu}^{II}$ with an additional row for component N_c. In contrast to this, the dimension of vectors $\mathbf{x}^{I}$ and $\mathbf{j}^{I}$ is the same, and is equal to the number of independent reactions.

In Eq. 32 the relation $J_{tot} = j_{tot}$ is used. This follows from the definition of J_{tot}

$$J_{\text{tot}} = \sum_{i=1}^{N_c-N_r} J_i = \sum_{i=1}^{N_c-N_r} \left(j_i - \sum_{j=1}^{N_r} \tilde{\boldsymbol{\nu}}_i^{II}(\boldsymbol{\nu}^{I})_j^{-1} j_j \right) \tag{34}$$

and the constant total mole number for each reaction according to

$$\sum_{i=1}^{N_c-N_r} \tilde{\boldsymbol{\nu}}_i^{II} = -\sum_{i=1}^{N_r} \boldsymbol{\nu}_i^{I} \tag{35}$$

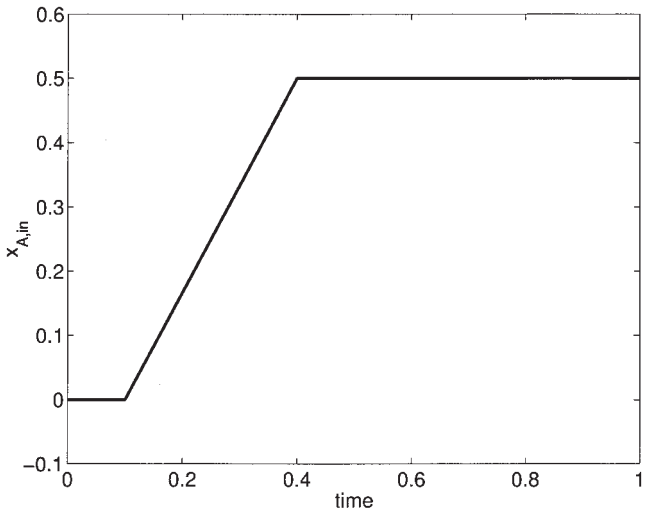

Figure 15. Ramp shaped input of concentration $x_{A,in}$ used for the startup scenarios in Figures 14, 16, 18.

respectively. The quantities $\tilde{\boldsymbol{\nu}}_i^{II}$, $\boldsymbol{\nu}_i^{I}$ represent the i-th row vector of the corresponding matrix and $(\boldsymbol{\nu}^{\mathrm{I}})_j^{-1}$ represents the j-th column vector of the corresponding inverse matrix. Hence

$$\sum_{i=1}^{N_c-N_r} j_i - \sum_{j=1}^{N_r} \tilde{\boldsymbol{\nu}}_i^{II}(\boldsymbol{\nu}^{I})_j^{-1} j_j = \sum_{i=1}^{N_c-N_r} j_i + \sum_{j=1}^{N_r} j_j = \sum_{i=1}^{N_c} j_i = j_{\mathrm{tot}} \tag{36}$$

Like in reactive distillation and reactive chromatography, the reactive problem in transformed concentration variables (Eq. 31), (Eq. 32) is completely analogous to the corresponding nonreactive problem (Eq. 27), (Eq. 28), and we can proceed in a similar way like in the previous section to investigate the qualitative behavior.

In a first step we will focus on a single reversible reaction of type $2A \rightleftharpoons B + C$. The treatment for the corresponding problems in reactive distillation and reactive chromatography was given by Grüner and Kienle.[1] In particular, it was shown that total conversion in an infinitely long column is only possible if reactant A has intermediate affinity to the vapor or the solid phase, respectively. In the other cases, achievable product compositions are limited by reactive azeotropy. Conditions for total conversion in a membrane reactor, however, are more restrictive. In this case total conversion of reactant A is only possible, if the membrane is not permeable at all for reactant A, and at least one of the products is continuously removed to shift the equilibrium to the product side. If, in addition, the membrane has zero permeability for the other product, simultaneous separation of the products is achieved. This situation is illustrated in Figure 16 with the transformed concentration and flux variables as introduced in Eq. 33. Therein, component A is taken as the reference, which leads to the following definitions

$$X_B = x_B + \frac{x_A}{2}, \quad X_C = 1 - X_B \tag{37}$$

$$J_B = j_B + \frac{j_A}{2}, \quad J_C = j_C + \frac{j_A}{2}$$

$$J_{tot} = J_A + J_B = j_A + j_B + j_C = j_{tot} \tag{38}$$

Furthermore, it is assumed in Figure 16 that the membrane is only permeable for product B, but not for product C.

For the simple system considered here, the flux rate ratio shown in Figure 16 can be calculated explicitly. It is equivalent to a reactive vapor liquid equilibrium with zero volatility for reactant A due to zero permeability of the membrane for this component. In the transformed concentration variables a value of X_B of zero corresponds to pure product C, a value of 0.5 to pure reactant A, and a value of 1 to pure product B. It should

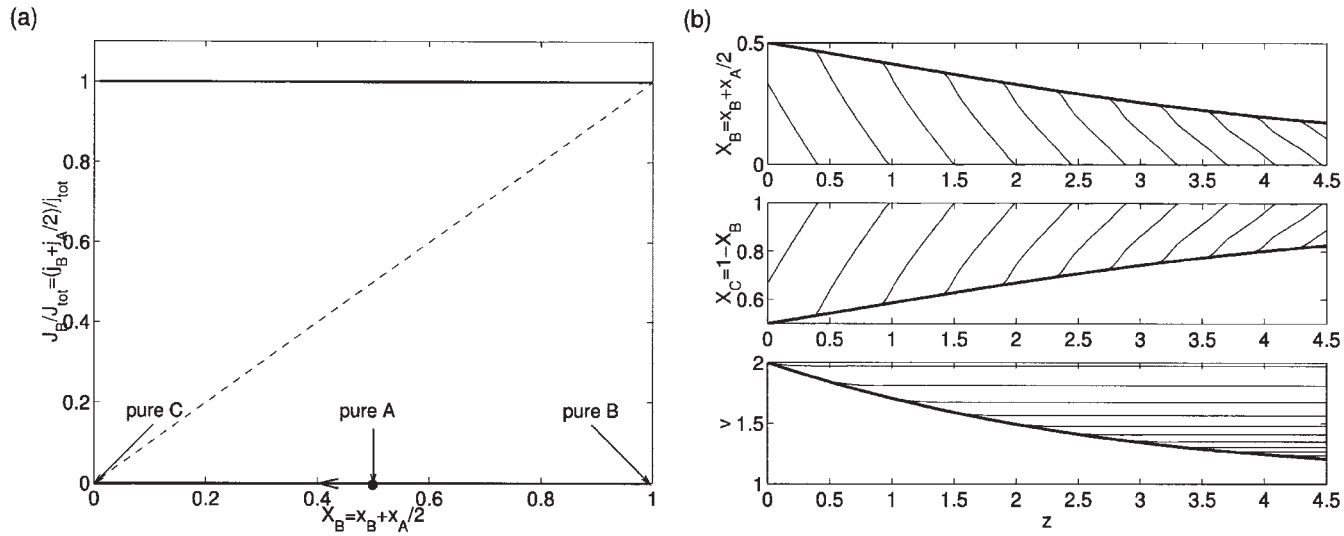

Figure 16. Membrane reactor with a reaction $2A \Leftrightarrow B + C$. Parameters: $\beta_A = \beta_C = 0$, $\beta_B = 1$, $K = 1$.

(a) Transformed flux rate ratio vs. X_B, (b) response to input ramp of $X_{B,in}$ or $x_{A,in}$, respectively, as shown in Figure 15. Thin lines = transient solutions at $t = 0.3, 0.6, \ldots, 3.3$, bold lines = steady state solution.

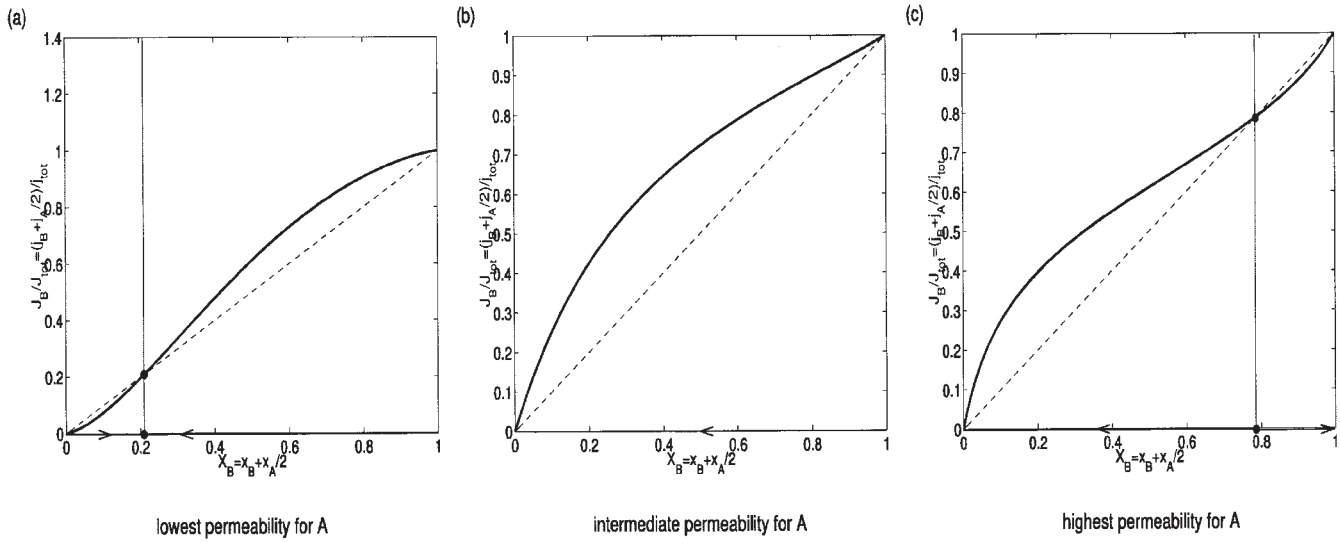

Figure 17. Membrane reactor with a reaction $2A \Leftrightarrow B + C$.

Parameters: $K = 1$, (a) $\beta_A = 1$, $\beta_B = 5$, $\beta_C = 3$, (b) $\beta_A = 3$, $\beta_B = 5$, $\beta_C = 1$, (c) $\beta_A = 5$, $\beta_B = 3$, $\beta_C = 1$.

be noted that the diagram on the left of Figure 16 has the same structural properties as the corresponding diagram of Figure 14, for the nonreactive binary case. In particular, the steady-state profile of X_B in the inner tube will monotonically decrease and tend to $X_B = 0$, which corresponds to pure product C in the inner tube. The dynamic transient behavior during startup is also analogous to the nonreactive case considered in Figure 14.

In practice, the membrane however often has finite permeability for all components, which is considered next. In this case the enhancement of the reaction through the membrane will strongly depend on the order of permeability of the membrane for the different components. In particular, three different cases will be considered, where the membrane has highest, intermediate or lowest permeability for reactant A. The permeability for B is assumed to be higher than for C in all three cases. Like in the previous case an explicit calculation of the transformed flux rate ratio is possible. The results are shown in Figure 17. These diagrams are exactly the same as the McCabe–Thiele diagrams for the corresponding ternary reactive distillation processes,[1] which are equivalent to McCabe–Thiele diagrams for binary nonreactive mixtures. The case with intermediate permeability corresponds to the nonreactive vapor liquid equilibrium of an ideal binary mixture, whereas the other two cases correspond to the nonreactive vapor liquid equilibrium of azeotropic binary mixtures. According to the terminology introduced by Huang et al.,[28] these "azeotropic points" will be called **reactive arheotropes** in the remainder. At these points the change of concentration through reaction and through mass transport across the membrane compensate each other and lead to constant composition. The corresponding profiles of the transformed concentration variables and the velocity v are shown in Figure 17. In the first case, the reactive arheotrope represents the maximum achievable composition which can be obtained in the inner tube of an infinitely long membrane reactor if the feed is pure reactant A. In the other two cases pure product C can be obtained in the inner tube. However, total conversion is of course not possible due to the loss of reactant across the membrane, due to the finite permeability for A. Again the qualitative dynamic behavior, which is illustrated in Figure 17 for a startup scenario, is completely analogous to the nonreactive case. In particular, in the first case the self sharpening characteristic of the traveling concentration fronts is very pronounced. Again, this comes from the decrease of the transport velocity from the entrance to the outlet.

An extension to multireaction and multicomponent systems with more than one independent variable is straight forward. Feasible products will follow from the corresponding reactive residue curve maps for membrane processes as introduced by Huang et al.[28] Propagation dynamics will follow from the variable transport velocity v, which is the same for all components. Step disturbances will therefore also in the reactive case

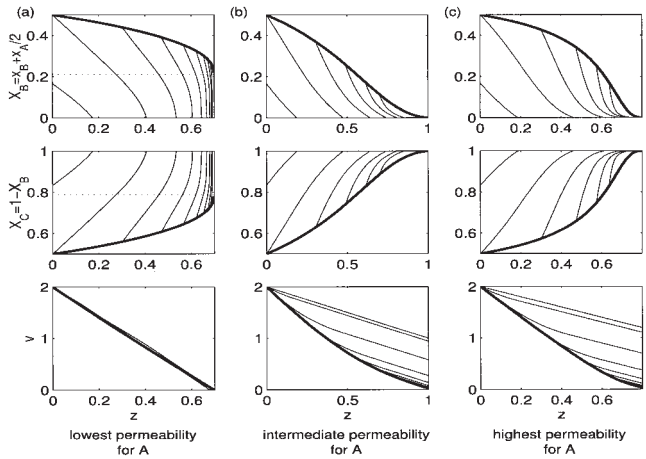

Figure 18. Membrane reactor with a reaction $2A \Leftrightarrow B + C$, response to input ramp of $X_{B,in}$ or $x_{A,in}$, respectively, as shown in Figure 15.

Thin lines = transient solutions at $t = 0.2, 0.4, \ldots, 1.2$, bold lines = steady state solution. (a) $\beta_A = 1$, $\beta_B = 5$, $\beta_C = 3$, (b) $\beta_A = 3$, $\beta_B = 5$, $\beta_C = 1$, (c) $\beta_A = 5$, $\beta_B = 3$, $\beta_C = 1$. Dotted lines in column (a) mark composition at the arheotropic point.

be resolved into a single wave traveling jointly for all (transformed) concentrations. The variable velocity v will result in self-sharpening waves.

Conclusion

In this article, a unifying approach for understanding the dynamic behavior of combined reaction separation processes with fast reversible chemical reactions was presented. It extends equilibrium theory, which was first applied to nonreactive chromatographic processes and nonreactive distillation processes to the reactive case.[10,23] The usefulness of the approach was illustrated for some fairly complex practical problems from the fields of reactive chromatography and reactive distillation. Furthermore, it was shown that an extension to membrane reactors is also possible. In the first two cases, phase equilibrium was assumed, whereas in the second case finite kinetics of the transport through the membrane were considered. Application of the theory is also possible for other process which fall in these classes. In particular, for the first class one could think of reactive extraction processes or sorption enhanced reaction processes. For the second class one could think of reactive pervaporation or of some other processes from the first class with nonnegligible transport resistance between the different phases. For a recent overview on other candidate processes we refer to Sundmacher et al.[5]

It was shown that the dynamic behavior of combined reaction separation processes with fast chemical reactions is equivalent to the dynamic behavior of the corresponding nonreactive problem in a reduced set of transformed concentration variables. This is consistent with the pioneering work of Doherty and co-workers for the corresponding steady-state problem in reactive distillation.[2,32] More specifically, it was shown that the dynamic behavior of these processes is governed by nonlinear wave propagation. These nonlinear waves provide a simple way for understanding the qualitative dynamics with little or even without any tedious calculations. Hence, they are a useful basis for further developments in the field of optimal operation and control of combined reaction separation processes. Possible applications are seen in similar fields like for nonreactive separation processes. In particular, concepts for nonreactive processes can be directly transferred to reactive processes by means of transformed concentration variables. These include nonlinear model reduction,[25] model based measurement and model based control,[33,34] like nonlinear model predictive control, for example. Furthermore, nonlinear waves may also guide the way to the development of new advanced operational strategies and new processes.[35–37]

In chromatography and membrane processes the extended equilibrium or nonlinear wave theory can be a useful tool for investigating feasibility and process design. In distillation and reactive distillation one might apply similar ideas for process design.[38] However, things are getting fairly complicated for highly nonideal mixtures, and there are other well established methods like residue curve maps available for this purpose.[39] Therefore, possible applications in the field of reactive distillation is mainly seen in process control.

The treatment in this article was based on some simplifying assumptions, which currently confine the applicability of the approach. As indicated in the section titled "Chromatographic Processes" an extension to variable flow rates for nonequimolar reactions which is straightforward in the steady state case[2,32] requires further careful investigation in the dynamic case. The reason is, that variable flow rates will directly affect the characteristic velocities. Hence, they will not only change the propagation velocity of the waves, but possibly also the wave types. Similar phenomena can be observed in nonreactive chromatography[40,41] and nonreactive distillation[42] if the overall flux across the phase boundary is not negligible compared to the convective transport in axial direction. Another interesting topic or further research is concerned with the influence of finite reaction kinetics on the dynamic behavior of combined reaction separation processes.

Acknowledgments

A. Kienle would like to thank Y. S. Huang for fruitful discussions on reactive pervaporation processes. The financial support of DFG (Deutsche Forschungsgemeinschaft) within the joint research projects SFB 412 on "Computer Aided Modeling and Simulation of Chemical Processes for Process Analysis, Synthesis and Operation" and FOR 447 on "Membrane Enhanced Reaction" is greatly acknowledged.

Notation

A = ratio of the molar flow rates in both phases
c_i = molar concentration in the fluid phase, kmol/m^3
C_i = transformed concentration variable of the fluid phase, kmol/m^3
j_i = dimensionless mass transfer rate
J_i = transformed flux variables
K_j = chemical equilibrium constant
l = length, m
N_c = number of components
N_s = number of solutes
N_r = number of reactions
q_i = molar concentration in the solid phase, kmol/m^3
Q_i = transformed concentration variable of the solid phase, kmol/m^3
r_j = dimensionless reaction rate
$\bar{r}_j$ = reaction rate, kmol/m^3
$\mathbf{r}$ = eigenvector
$\bar{t}$ = time, s
t = dimensionless time
v = dimensionless velocity
x_i = mole fraction of the liquid phase
X_i = transformed concentration variable of the liquid phase
y_i = mole fraction of the vapor phase
Y_i = transformed concentration variable of the vapor phase
$\bar{z}$ = spatial coordinate, m
z = dimensionless spatial coordinate

Greek letters

α_i = constant relative volatility
β_i = dimensionless transport coefficient through the membrane
ε = ratio of the molar holdups in both phases
λ = eigenvalue
ν_{ij} = stoichiometric coefficients
ν = volume ratio of solid and fluid phase
μ = volumetric flow ratio of solid and fluid phase

Subscripts and superscripts

i, k = species
j = reaction
in = input
tot = total
$'$ = Phase ($'$)
$''$ = Phase ($''$)

Literature Cited

1. Grüner S, Kienle A. Equilibrium theory and nonlinear waves for reactive distillation columns and chromatographic reactors. *Chem Eng Sci.* 2004;59:901–918.
2. Barbosa D, Doherty MF. A new set of composition variables for the representation of reactive phase diagrams. *Proc R Soc Lond.* 1987; A413:459–464.
3. Kulprathipanja S. *Reactive Separation Processes.* New York: Taylor & Francis; 2002.
4. Sundmacher K, Kienle A. *Reactive Distillation—Status and Future Trends.* Weinheim: Wiley-VCH; 2003.
5. Sundmacher K, Kienle A, Seidel-Morgenstern A. *Integrated Chemical Processes.* Weinheim: Wiley-VCH; 2005.
6. Gaikar VG, Sharma MM. Separations through reactions and other novel strategies. *Sep Purif Meth.* 1989;18:111–176.
7. Kienle A, Marquardt W. Nonlinear dynamics and control of reactive distillation processes. In: Sundmacher K, Kienle A, Eds. *Reactive Distillation—Status and Future Directions.* Weinheim: Wiley-VCH, 2003;241–281.
8. Helfferich FG, Klein G. *Multicomponent Chromatography. Theory of Interference.* New York: M. Dekker; 1970.
9. Rhee H-K, Aris R, Amundson NR. *First-Order Partial Differential Equations: Volume I—Theory and Application of Single Equations.* New Jersey: Prentice Hall; 1986.
10. Rhee H-K, Aris R, Amundson NR. *First-Order Partial Differential Equations: Volume II—Theory and Application of Hyperbolic Systems of Quasilinear Equations.* New Jersey: Prentice Hall; 1989.
11. Ung S, Doherty MF. Calculation of residue curve maps for mixtures with multiple equilibrium chemical reactions. *Ind Eng Chem Res.* 1995;34:3195–3202.
12. Aiouache F, Goto S. Sorption effect on kinetics of etherification of tert-amyl alcohol and ethanol. *Chem Eng Sci.* 2003;58:2065–2077.
13. Helfferich FG, Carr PW. Nonlinear-waves in chromatography. 1. Waves, shocks, and shapes. *J Chromatogr A.* 1993;629:97–122.
14. Helfferich FG, Whitley RD. Nonlinear-waves in chromatography. 2. Wave interference and coherence in multicomponent systems. *J Chromatogr A.* 1996;734:7–47.
15. Helfferich FG. Non-linear waves in chromatography. 3. Multicomponent Langmuir and Langmuir-like systems. *J Chromatogr A.* 1997; 768:169–205.
16. Basmadjian D, Coroyannakis P. Equilibrium-theory revisted—Isothermal fixed-bed sorption of binary systems. 1. Solutes obeying the Langmuir isotherm. *Chem Eng Sci.* 1987;42:1723–1735.
17. Basmadjian D, Coroyannakis P, Karayannopoulos C. Equilibrium-theory revisted—Isothermal fixed-bed sorption of binary systems. 2. Non-Langmuir solutes with type I parent isotherms—Azeotropic systems. *Chem Eng Sci.* 1987;42:1737–1752.
18. Basmadjian D, Coroyannakis P, Karayannopoulos C. Equilibrium-theory revisited—Isothermal fixed-bed sorption of binary systems. 3. Solutes with type I, type II and IV parent isotherms—Phase-separation phenomena. *Chem Eng Sci.* 1987;42:1753–1764.
19. Baciocchi R, Zenoni G, Mazzotti M, Morbidelli M. Separation of binaphtol enantiomers through achiral chromatography. *J Chromatogr A.* 2002;944:225–240.
20. Nicoud RM, Jaubert JN, Rupprecht I, Kinkel J. Enantiomeric enrichment of non-racemic mixtures of binaphthol with non-chiral packings. *Chirality.* 1996;8:234–243.
21. Baciocchi R, Mazzotti M, Morbidelli M. A general model for the achiral chromatography of enantiomers froming dimers: Application to binaphthol. *J Chromatogr A.* 2004;1024:15–20.
22. Schaeffer DG, Schearer M. The classification of 2×2 systems of non-strictly hyperbolic conservation laws, with application to oil recovery. *Comm Pure Appl Math.* 1987;XL:141–178.
23. Kienle A. *Nichtlineare Wellenphänomene und Stabilität stationärer Zustände in Destillationskolonnen.* VDI Fortschritt-Berichte Nr. 3/506Düsseldorf: VDI-Verlag; 1997.
24. Kienle A, Marquardt W. Bifurcation analysis and steady-state multiplicity of multicomponent, non-equilibrium distillation processes. *Chem Eng Sci.* 1991;46:1757–1769.
25. Kienle A. Low-order dynamic models for ideal multicomponent distillation processes using nonlinear wave propagation theory. *Chem Eng Sci.* 2000;55:1817–1828.
26. Doherty MF, Perkins JD. On the dynamics of distillation processes—I. The simple distillation of multicomponent nonreacting, homogeneous liquid mixtures. *Chem Eng Sci.* 1978;33:281–301.
27. Mai PT, Vu TD, Mai KX, Seidel-Morgenstern A. Analysis of heterogeneously catalyzed ester hydrolysis performed in a chromatographic reactor and in a reaction calorimeter. *Ind Eng Chem Res.* 2004;43: 4691–4702.
28. Huang YS, Sundmacher K, Qi Z, Schlünder EU. Residue curve maps of reactive membrane separation. *Chem Eng Sci.* 2004;59:2863–2879.
29. Coronas J, Santamaria J. Catalytic reactors based on porous ceramic membranes. *Catalysis Today.* 1999;51:377–389.
30. Krishna R, Wesselingh JA. The Maxwell–Stefan approach to mass transfer. *Chem Eng Sci.* 1997;52:861–911.
31. Fullarton D, Schlünder EU. Diffusion distillation—A new separation process for azeotropic mixtures. 1. Selectivity and transfer efficiency. *Chem Eng Proc.* 1986;20:255–263.
32. Ung S, Doherty MF. Synthesis of reactive distillation systems with multiple equilibrium chemical reactions. *Ind Eng Chem Res.* 1995;34: 2555–2565.
33. Grüner S, Mohl KD, Kienle A, Gilles ED, Fernholz G, Friedrich M. Nonlinear control of an industrial reactive distillation column. *Contr Eng Practice.* 2003;11:915–925.
34. Grüner S, Schwarzkopf S, Uslu I, Kienle A, Gilles ED. Nonlinear model predictive control of multicomponent distillation columns using wave models 2003. *Proc 7th International Symposium on Advanced Control of Chemical Processes.* Vol. 1, Hong Kong, China, 2004;01-11:231–236.
35. Kienle A, Lauschke G, Gehrke V, Gilles ED. On the dynamics of the circulation loop reactor—Numerical methods and analysis. *Chem Eng Sci.* 1995;50:2361–2375.
36. Schramm H, Kaspereit M, Kienle A, Seidel-Morgenstern A. Simulated moving bed process with cyclic modulation of the feed concentration. *J Chromatogr A.* 2003;1006:77–86.
37. Schramm H, Kaspereit M, Kienle A, Seidel-Morgenstern A. Improved operation of simulated moving bed process through cyclic modulation of feed flow and feed concentration. *Chem Eng Sci.* 2003;58:5217–5227.
38. Mazzotti M, Storti G, Morbidelli M. Multicomponent distillation design through equilibrium theory. *Ind Eng Chem Res.* 1998;37:2250–2270.
39. Doherty MF, Malone MF. *Conceptual Design of Distillation Systems.* New York: McGraw-Hill; 2001.
40. Peterson DL, Helfferich F. Towards a generalzied theory of gas chromatography at high solute concentrations. *J Phys Chem.* 1969;65: 1283–1293.
41. LeVan MD, Costa CA, Rodrigues AE, Bossy A, Tondeur DM. Fixed-bed adsorption of gases—Effect of velocity variations on transition types. *AIChE J.* 1988;34:996–1005.
42. Marquardt W. *Nichtlineare Wellenausbreitung—ein Weg zu reduzierten Modellen von Stofftrennprozessen.* VDI Fortschrittsberichte Nr. 8/161Düsseldorf: VDI-Verlag; 1988.
43. Brenan KE, Campbell SL, Petzold LR. *Numerical Solution of Initial Value Problems in Differential-Algebraic Equations.* North Holland & Elsevier Science Publishing Company; 1989.

Appendix A

Calculation of the pathgrid of the transformed equilibrium function

The construction of wave solutions for chromatographic reactors and reactive distillation processes is based on the pathgrid of the eigenvectors of the Jacobians $\partial \mathbf{Q}(\mathbf{C})/\partial \mathbf{C}$ and $\partial \mathbf{Y}(\mathbf{X})/\partial \mathbf{X}$ of the transformed equilibrium functions $\mathbf{Q}(\mathbf{C})$ and $\mathbf{Y}(\mathbf{X})$ defined by Eqs. 8 and 19. For most systems the computation of this Jacobian is not directly possible since the transformed equilibrium functions are not explicitly known, but only implicitly. In the following it is shown how to compute the Jacobian $\partial \mathbf{Q}(\mathbf{C})/\partial \mathbf{C}$ by implicit differentiation in terms of the known derivatives of the adsorption isotherms and the reaction equilibrium. The procedure for $\partial \mathbf{Y}(\mathbf{X})/\partial \mathbf{X}$ is analogous and will, therefore, not be discussed in detail.

For chromatographic reactors the transformed equilibrium function is defined according to Eq. 8 by

$$\mathbf{Q} = \mathbf{q}^{II} - \boldsymbol{\nu}^{II}(\boldsymbol{\nu}^{I})^{-1}\mathbf{q}^{I} \tag{A1}$$

The solid phase concentration vectors $\mathbf{q}^{I}$ and $\mathbf{q}^{II}$ in this definition are related to the fluid phase concentration vector $\mathbf{c}$ by the adsorption isotherm. Furthermore, the fluid phase concentration vector $\mathbf{c}$ is related implicitly to the transformed fluid phase concentration vector $\mathbf{C}$ by definition (Eq. 8) and N_r additional algebraic constraints for chemical equilibrium of all chemical reactions according to

$$\mathbf{0} = \mathbf{F}(\mathbf{c}, \mathbf{C}) = \begin{pmatrix} \mathbf{C} - \mathbf{c}^{II} + \boldsymbol{\nu}^{II}(\boldsymbol{\nu}^{I})^{-1}\mathbf{c}^{I} \\ \mathbf{f}(\mathbf{c}) \end{pmatrix} \tag{A2}$$

Here, the function vector $\mathbf{f}(\mathbf{c})$ represents the chemical equilibrium constraints. For an ideal mixture, these equilibrium conditions are

$$0 = f_k(\mathbf{c}) = K_k - \prod_{i=1}^{N_s} c_i^{\nu_{ik}}, \quad k = 1, \ldots N_r \tag{A3}$$

for example. In Eqs. A.2 and A.3, it is implicitly assumed that the chemical reactions take place in the fluid phase as in the binaphthol application example considered earlier. However, it should be noted, that an analogous procedure is possible if the chemical reactions take place in the solid phase. Equation A.2 represent N_s implicit equations for calculating N_s unknown c_i's from $N_s - N_r$ transformed concentration variables C_i.

Now, the required Jacobian $\partial\mathbf{Q}(\mathbf{C})/\partial\mathbf{C}$ is obtained by differentiation of Eq. A.1 with respect to $\mathbf{C}$ according to

$$\frac{\partial \mathbf{Q}}{\partial \mathbf{C}} = \frac{\partial \mathbf{Q}}{\partial \mathbf{c}} \frac{\partial \mathbf{c}}{\partial \mathbf{C}} \tag{A4}$$

In this expression, the derivative $\partial\mathbf{Q}/\partial\mathbf{c}$ involves the standard derivatives of the adsorption isotherms with respect to the fluid phase concentrations according to

$$\frac{\partial \mathbf{Q}}{\partial \mathbf{c}} = \frac{\partial}{\partial \mathbf{c}} \left(\mathbf{q}^{II} - \boldsymbol{\nu}^{II}(\boldsymbol{\nu}^{I})^{-1}\mathbf{q}^{I}\right) \tag{A5}$$

and the derivative $\partial\mathbf{c}/\partial\mathbf{C}$ is obtained by implicit differentiation of Eq. A.2

$$\frac{\partial \mathbf{c}}{\partial \mathbf{C}} = -\left(\frac{\partial \mathbf{F}}{\partial \mathbf{c}}\right)^{-1} \frac{\partial \mathbf{F}}{\partial \mathbf{C}} \tag{A6}$$

The pathgrid is computed by integrating along the eigenvectors $\mathbf{r}_k(\mathbf{C})$ of the Jacobian A.4–A.6, for suitable initial conditions according to

$$\frac{d\mathbf{C}}{d\xi} = \mathbf{r}_k(\mathbf{C}), \quad \mathbf{C}(\xi = 0) = \mathbf{C}_0 \tag{A7}$$

The independence variable ξ in this equation represents some suitable parametrization of the curve in the hodograph space.

Since the derivatives in Eqs. A.4–A.6 also depend on the original fluid phase concentration vector $\mathbf{c}$, $\mathbf{c}$ has to be determined simultaneously for each value of $\mathbf{C}$ along the curve from the implicit algebraic Eq. A.2. This is done most conveniently with a DAE solver like DASSL for example.[43] Since DASSL is available in MATLAB, a program for calculating and visualizing the pathgrid is readily implemented in MATLAB.

Manuscript received July 23, 2004, and revision received July 23, 2005.